



CHORUS

This is the accepted manuscript made available via CHORUS. The article has been published as:

Black hole mass function from gravitational wave measurements

Ely D. Kovetz, Ilias Cholis, Patrick C. Breysse, and Marc Kamionkowski

Phys. Rev. D **95**, 103010 — Published 30 May 2017

DOI: [10.1103/PhysRevD.95.103010](https://doi.org/10.1103/PhysRevD.95.103010)

The Black Hole Mass Function from Gravitational Wave Measurements

Ely D. Kovetz, Ilias Cholis, Patrick C. Breysse and Marc Kamionkowski

Department of Physics and Astronomy, Johns Hopkins University, Baltimore, MD 21218 USA

We examine how future gravitational-wave measurements from merging black holes (BHs) can be used to infer the shape of the black-hole mass function, with important implications for the study of star formation and evolution and the properties of binary BHs. We model the mass function as a power law, inherited from the stellar initial mass function, and introduce lower and upper mass cutoff parameterizations in order to probe the minimum and maximum BH masses allowed by stellar evolution, respectively. We initially focus on the heavier BH in each binary, to minimize model dependence. Taking into account the experimental noise, the mass measurement errors and the uncertainty in the redshift-dependence of the merger rate, we show that the mass function parameters, as well as the total rate of merger events, can be measured to $< 10\%$ accuracy within a few years of advanced LIGO observations at its design sensitivity. This can be used to address important open questions such as the upper limit on the stellar mass which allows for BH formation and to confirm or refute the currently observed mass gap between neutron stars and BHs. In order to glean information on the progenitors of the merging BH binaries, we then advocate the study of the two-dimensional mass distribution to constrain parameters that describe the two-body system, such as the mass ratio between the two BHs, in addition to the merger rate and mass function parameters. We argue that several years of data collection can efficiently probe models of binary formation, and show, as an example, that the hypothesis that some gravitational-wave events may involve primordial black holes can be tested. Finally, we point out that in order to maximize the constraining power of the data, it may be worthwhile to lower the signal-to-noise threshold imposed on each candidate event and amass a larger statistical ensemble of BH mergers.

I. INTRODUCTION

Black holes (BHs) were first identified as a solution to Einstein’s field equations by Schwarzschild in 1916 [1]. As early as 1939 it was demonstrated that, in principle, they can be formed by the collapse of stars [2, 3]. Many decades later, numerous advances have been made in the study of the physics of black hole formation from stars—either by direct collapse or through fallback from supernova explosions—and core-collapse simulations have been developed to include more and more of the relevant mechanisms, most notably the delayed neutrino-driven explosion mechanism [4, 5]. However, the theory still lacks a clear prediction for the number and mass distribution of stellar-mass BHs in the Universe [6–10].

Observationally, evidence for the existence of stellar-mass BHs in nature has only recently started to accumulate, thanks to indirect observations of X-ray emission from accretion of matter from their binary star companions [11–16]. To date, less than two dozen stellar-mass BHs have been detected in this way, most of them in the Milky Way, with a handful of extragalactic candidates [17, 18]. These X-ray observations, however, are limited in reach, becoming more biased as the distance from Earth grows, and do not allow a meaningful sample to be gathered in order to test the black hole mass function (BHMF) on cosmological scales.

Unfortunately, as their name suggests, black holes do not emit electromagnetic radiation and cannot be directly seen. They can be directly *heard*, however, through gravitational wave (GW) emission from their interaction with binary companions such as other black holes and neutron stars [19–23] (or from close fly-by encounters,

such as tidal disruption events [24–27]). The associated time-varying mass quadrupole moment of the two-body system results in the emission of GWs, as predicted by Einstein [28]. These (weak) GW signals have long been sought after in dedicated experiments, culminating in the announcement of the first discovery of a coalescing black hole binary earlier this year by the LIGO observatory [29].

With this and subsequent detections of additional binary black hole (BBH) mergers [30, 31], the era of gravitational wave astronomy has now finally begun. Overall, advanced LIGO in its 2015 O1 run observed three¹ BH coalescence events, adding nine additional measured black hole masses to the current data (the six pre-merger masses range from roughly 7 to $36 M_{\odot}$). Over the next decade, improvements in detector sensitivities are expected to usher in a wave of newly detected events. LIGO itself is scheduled to perform two more runs (O2,3) with increasing sensitivity before commencing a multi-year run at its design sensitivity at the turn of the decade. Meanwhile, VIRGO [32] is scheduled to start observing during 2017, and plans exist for additional detectors to be built in Japan [33, 34] and India [35] as well. These experiments will lead to the discovery of many hundreds of merger events per year, providing a rich dataset of black hole statistics to investigate.

In this paper, we demonstrate that the detection of gravitational waves from thousands of black hole merger events over the next decade will transform our knowl-

¹ The event denoted by LVT151012 has a 1.7σ significance, with an estimated 87% Bayesian probability to have been a BBH merger.

edge of the black hole mass distribution, which in turn will shed new light on the study of stellar evolution (and termination), star formation history, and the progenitor models of binary black holes. We show, for instance, that the relation between the slope of the BHMF and the stellar initial mass function (IMF) can be probed with high precision. We pay particular attention to the measurement of the tails of the mass distribution. This can weigh in on pressing issues such as the empirical hints of a mass gap between neutron stars and black holes [36, 37] and the abundance of the most massive stellar black holes, which is limited by processes such as wind-driven mass loss [38], preventing the heaviest stars from retaining their masses until they collapse to form black holes. We then demonstrate that characterizing the distribution of the mass ratio between the BBH constituents can be used to probe the efficiency and counterbalance of different binary formation mechanisms showing that certain models, such as primordial black holes making up the dark matter in our Universe [39], can be significantly constrained and possibly ruled out with several years of observation.

Our paper is constructed as follows: In Section II we describe our assumptions for the BH mass function and its relation to several types of BBH models. Section III provides the details of our analysis, including details on the choice of parameters and noise curves for the future experiments that we consider. Our results are presented and explained in Section IV. Various subtleties and suggestions for future work are discussed in Section V. We conclude in Section VI.

II. MODELING THE BH MASS FUNCTION

A. The stellar initial mass function

In this work our reference assumption is that all BHs with mass less than $\sim 100 M_\odot$ originate from the demise of massive stars (i.e. unless stated otherwise, we neglect previous mergers, primordial black holes, etc.). To this day, only 29 such BHs have been detected. These include 23 BHs discovered through X-rays, 18 of which are galactic (see [17, 40, 41] and references therein) and five extragalactic [18, 42–46]. The remaining ones were recently detected through the gravitational waves released from the merger of BBHs with masses between 7 to $36 M_\odot$ into even more massive end products (in total six pre-merger BHs in three merger events) [29–31]. In addition, there are 42 X-ray transients within the Milky Way that are candidates for hosting BHs [17].

Given the currently limited data, in order to model the BHMF, we choose to use the better constrained initial mass function (IMF) for stars [47, 48]. The stellar IMF is well-described by a multi-part power-law $P(M) \propto M^{-\alpha}$, with α taken to be 2.3 ± 0.7 for $M > 1 M_\odot$ [48]. Since the stellar BHs we are concerned with originate from stars with initial mass $\gtrsim 20 M_\odot$, we are only sensitive to the

slope in the higher mass range. We therefore assume for simplicity that the more massive BHs in each binary, whose mass we denote by M_1 , will also follow a power-law mass distribution $P_{\text{BH}}(M_1) \propto M_1^\alpha$, with the value of α corresponding to the relevant mass range for the progenitor stars. We note that the true relation between the progenitor star mass and the black hole mass may very well be more complex than assumed here [49–52].

To facilitate a comparison with the LIGO collaboration results in Ref. [31], where a power-law BHMF inherited from the IMF was also postulated, we follow their assumptions and set $\alpha = 2.35$ as our fiducial value. We will examine the precision with which α can be constrained by advanced LIGO observations over the coming decade (assuming a power-law distribution remains consistent with the data). After the first observations of the three coalescence events GW150914, LVT151012 and GW151226, LIGO has constrained α to be $2.5_{-1.6}^{+1.5}$ at 90% credible interval. We shall see that future observations will go well beyond this precision.

B. Endpoints in the mass function of BHs: the mass gap and mass cap

The boundary mass between a neutron star (NS) and a BH is expected not to exceed $M \simeq 3 M_\odot$, with Ref. [53] suggesting a value of $2.5 M_\odot$ as the highest possible neutron star mass. In current observations, the most massive well-measured neutron star is $2.01 \pm 0.04 M_\odot$ [54] and the least massive BH is $\sim 4.4 M_\odot$ [55]. This has led various authors to suggest the presence of a mass gap between approximately $2\text{--}5 M_\odot$ [36, 37, 56]. It remains to be seen whether this empirical mass gap originates from selection effects in the still small sample of BHs (although based on the IMF, we would expect lower-mass BHs to be more abundant), or from the underlying assumptions that enter into their mass estimates [57], or whether it is indeed suggestive of the properties of the relevant supernovae and their progenitor stars [10, 38, 58]. Our results below will show that the mass gap, especially if the transition is as sharp as currently indicated by both experiment and pertaining theoretical models, can be extremely well constrained by gravitational wave measurements.

Meanwhile, we also expect an upper bound on the stellar mass allowing for BH formation. Wind-driven mass loss causes stars too massive to lose a significant portion of their mass before they evolve to produce black holes [59] (see though Ref. [60]). Stars heavier than $\sim 300 M_\odot$ have not been observed to date [61]. Meanwhile, various works (see e.g. Refs. [62–66]) have suggested a lower and more conventional upper bound on the stellar mass $\simeq 150 M_\odot$). We wish to explore the sensitivity of GW measurements to this important quantity.

We therefore parametrize the BHMF as

$$P(M_1) \propto M_1^{-\alpha} \mathcal{H}(M_1 - M_{\text{gap}}) e^{-M_1/M_{\text{cap}}} \quad (1)$$

where M_1 is the mass of the heavier binary component,

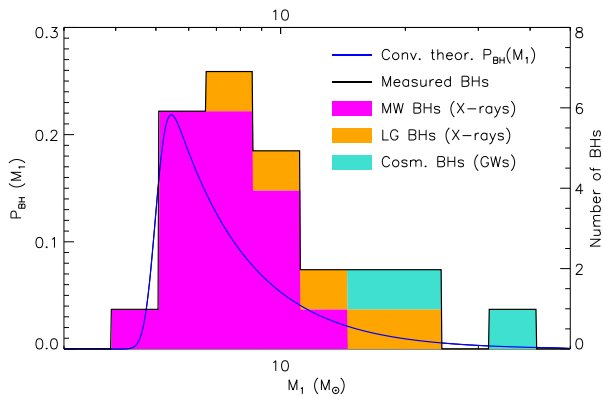


FIG. 1. The distribution function $P_{\text{BH}}(M_1)$ of the heavier BH mass M_1 in either BBHs or BH-star binaries. The blue line shows the theoretical prediction of Eq. (1) convolved with a Log Normal distribution that has a 5% error. The black histogram describes the observed distribution from 26 BHs. The red histogram is similar, but is based solely on the 18 dynamically confirmed BHs observed in X-rays that originate in the Milky Way. The yellow histogram stacked on the red one includes the five BHs observed through X-rays at LMC, IC 10, M33 and NGC 300. The green histogram stacked on the other two includes the three M_1 masses detected by LIGO.

α is a power law with a fiducial value of 2.35 (to match the Kroupa mass function [48]), M_{gap} is the NS-BH transition cutoff, which we take to be sharp, M_{cap} is a (shallower) exponential upper cutoff on the BH mass and \mathcal{H} is the Heaviside function.

In Fig. 1, we plot the mass distribution of BHs observed in X-ray binaries as well as merging BBHs. For the latter we only show the mass of the heaviest of the two BHs M_1 (before the merger event). We divide the X-ray binaries to Galactic (denoted by MW) and extragalactic events that have been detected in the Local Group or in its direct vicinity (denoted by LG). For the more distant X-ray binaries there is some selection effect towards more massive systems. In solid blue we plot the theoretical probability density function of M_1 , Eq. (1). To account for reasonable uncertainty in the mass estimation, we convolve the BHMF with a log-normal distribution with a 5% error in the mass (see more on the treatment of mass measurement errors in the next section).

While the statistics based on GW measurements in this figure are quite modest, we expect up to thousands of BBHs to be observed in the next decade. These observations will surpass the X-ray sample in size by a significant factor and as we demonstrate will dramatically affect the observed mass distribution.

C. Redshift-dependence of BH-BH merger rates

In addition to learning about the distribution of BH masses, inferring their local merger rate and their redshift

distribution is of great interest. X-ray observations have resulted in the detections of X-ray transients from binaries with a BH and a companion star that extend only as far away as NGC 300 (just in the vicinity of the Local Group, at a distance of 1.8 Mpc [67]), with the majority of transients detected inside the Milky Way. Looking forward, with gravitational wave measurements we will be able to probe merger events of BH binaries at cosmological distances up to Gpc, or in terms of redshift up to $z \sim 0.3$ with the current instrumental sensitivity [68] and up to $z \simeq 1$ with the expected advanced LIGO design [69]. In the future, experiments such as the Einstein Telescope (ET) may reach detection thresholds corresponding to redshifts $z \gtrsim 10$ [70].

After the first three detections, the local rate of BBH mergers has been estimated by LIGO to be 53_{-40}^{+100} $\text{Gpc}^{-3}\text{yr}^{-1}$, assuming that the three events do not follow any specific mass function, and 99_{-70}^{+138} $\text{Gpc}^{-3}\text{yr}^{-1}$ if their heaviest mass m_1 follows a mass function scaling as $M_1^{-2.35}$ down to masses of $5 M_{\odot}$ [31]. This rate is not expected to be redshift independent and instead is sensitive to the metallicity environment in which BBHs form, as well as the typical timescale for them to merge. This timescale is referred to as the time delay. For stellar BBHs it is of the order of 100s of Myrs to Gyrs (see Ref. [71] and references therein). If BBHs originate mainly in low metallicity environments, their merger rates $R(z)$ peak at high redshifts, while if the time delay is large, that peak moves to lower z .

With the cosmological distances $z \simeq 1$ to be probed in the next decade, it is preferable to use a generic parametrization that accounts both for the local rate uncertainties and for the uncertainties in the redshift distribution. In this work we use a simplified parametrization given by

$$R(z) = R_a(1+z)^{R_b}. \quad (2)$$

This monotonic behavior of $R(z)$ cannot be valid up to arbitrarily high values of z . If most BBH systems form in high metallicity environments, then with sufficient LIGO observations we should see a deviation from this parametrization, leading to lower best-fit values for R_b . Furthermore, even for very low metallicity environments and ignoring any time delays, $R(z)$ is expected to drop for $z > 4$ [9, 71]. Thus, Eq. (2) can be considered relevant only for the BBH coalescence observations from Advanced LIGO. With ET sensitivities, for example, such a parametrization will require modifications, to account for the decreasing merger rate at high redshifts.

For this work, we take as fiducial values for R_a a local rate of $99 \text{ Gpc}^{-3}\text{yr}^{-1}$ and for the power-law index R_b a value of 2. These provide a good fit to the approximations in Ref. [9]. In our analysis of the BHMF below, we will either hold the rate parameters fixed—an optimistic assumption—or marginalize over them—which is a conservative assumption, appropriate if there is no other source (based on theory or experiment) to provide more information. Our constraints on the merger rate param-

eters themselves are calculated when marginalizing over the other parameters, to avoid additional assumptions that are often made in the analysis (such as in Ref. [31]).

D. The mass ratio in BBHs and the 2D BHMF

The measurement of the mass of the lighter black hole in the merging binaries presents both a challenge and an opportunity. On the one hand, it would double the amount of information that can in principle be used to infer the BHMF parameters. On the other hand, this requires the two-dimensional distribution of the masses in the binary, which is strongly model dependent. Binary formation mechanisms vary greatly in their prediction for the binary mass ratio $q \equiv M_2/M_1$.

In the common envelope scenario, where the BHs are formed from binary stars which subsequently transform into BHs, with mass exchanged between the two throughout their common evolution [72], we expect the ratio to be larger than it would be under the naive assumption that the mass values for both M_1 and M_2 are drawn randomly from the same distribution ($\propto M^{-\alpha}$) [7, 73, 74]. In this scenario, the BH masses depend also on how effective the Wolf-Rayet phase is, during which significant mass loss of the progenitor stars takes place.

Dynamical formation of binaries tends to lead to larger values of q [75, 76]. One of the reasons is dynamical friction. In globular clusters and in environments where the BHs fall towards the center of a potential, it causes the most massive BHs to fall in first, and thus the first binaries to form in/close to the center of the potential are the pairs that contain the most massive BHs. Then the next most massive stars fall in and create companions, etc. Another reason to expect high values of q is scattering processes, either involving the BBH and an additional single BH, or between two BBHs. Simulations have shown that in dense environments, binaries tend to exchange components, preferentially ejecting their smaller partners in favor of more massive companions [76–78].

Meanwhile, more exotic mechanisms may lead to more extreme q distributions. In the primordial black hole scenario, for example, observational constraints limit the extent of the mass function and if the mass distribution is narrow, we expect q to be roughly unity for all PBH binaries. In this case, of course, the 2D distribution would be very different than for stellar black holes, as both masses would have similarly narrow distributions. We shall return to this point below.

We therefore describe the 2D BHMF using Eq. (1) and

$$P(M_2) \propto (M_2/M_1)^\beta \mathcal{H}(M_2 - M_{\text{gap}}) \mathcal{H}(M_1 - M_2), \quad (3)$$

where M_2 is the mass of the lighter binary component and β is a power law with a value that depends on the BBH progenitor model. As a fiducial value we follow the LIGO analysis in their Ref. [31] and set $\beta = 0$, i.e. a uniform distribution for M_2 in the range $[M_{\text{gap}}, M_1]$. In

order to provide a result that is less progenitor-model dependent, however, we differ from the analysis in Ref. [31] in that rather than *fixing* this assumption for the probability distribution of the lighter mass in each binary, we first limit the analysis to contain only the number counts of the heavier mass in each binary and calculate the constraints on the BHMF parameters while *marginalizing* over the mass ratio parameter introduced in Eq. (3). As explained below, we then extend our analysis to use the full two-dimensional mass distribution and constrain the mass ratio in tandem with the BHMF parameters.

III. ANALYSIS

A. Experimental signal-to-noise ratio

The detectability of GWs from a coalescence event depends on the relevant signal-to-noise ratio (S/N), which for a single interferometer detector is given by

$$(S/N)^2 = \frac{4}{5} \int_{f_{\text{min}}}^{f_{\text{max}}} df \frac{h_c^2(f)}{S_n(f)(2f)^2}, \quad (4)$$

where $h_c(f)$ is the observed strain amplitude and $S_n(f) = h_n^2(f)$ is the strain noise amplitude. We follow the same assumptions and parametrization of the coalescence signal from two merging BHs of Ref. [79] (see references therein), including though only the dominant quadrupole radiation. We assume that a given event is “detected” when the S/N in a single interferometer satisfies

$$S/N > 8.0. \quad (5)$$

This single detector criterion approximately translates into $S/N > 12$ for a network of the two LIGO detectors and given the overall lower sensitivity of the VIRGO interferometer is roughly correct for the combination of the three as well. This criterion is conventionally used as the threshold for a GW detector network to be able to identify the GW signal from a merging binary (e.g. [80]).

Since a large sample of events is necessary in order to understand the averaged properties of BBHs over cosmological distances, we will also consider less stringent S/N thresholds for the flagging of candidate GW events as detected mergers. The inevitable tradeoff between more statistics and larger individual mass estimation errors may motivate future advances in the estimation of the component BH masses in the binaries. To decouple our reported forecasts from our noise-related assumptions (we neglect the observing duty cycle of the experiment, for example), our main results will be presented in terms of the total number of detected coalescence events (for bookkeeping purposes, we will quote the corresponding number of observation years under our assumptions). Imposing a lower S/N threshold will simply result in attaining the same sample size earlier in time (and vice versa). The noise power spectrum used in our calculations refers

to advanced LIGO in its final design sensitivity, for which we adopt a noise model based on the analytical approximation of Ref. [23] (see their Eq. (4.7)) to the official advanced LIGO design noise curve [81]. We set the lower frequency limit at $f_{\min} = 20$ Hz, above which these noise curves match very well.

B. Mass measurement error

In order to account for errors in the individual masses, we use two methods. First, we assume a relative error in the mass measurement and so to get the *observed* probability distribution function, we convolve Eq. (1) with a log-normal distribution

$$\begin{aligned} P(M_{\text{obs}}) &= \iint P(M_{\text{th}}) P_G(x) \delta(M_{\text{obs}} - xM_{\text{th}}) dx dM_{\text{th}} \\ &= \int P(M_{\text{th}}) P_G(M_{\text{obs}}/M_{\text{th}}) dM_{\text{th}}/M_{\text{th}} \end{aligned} \quad (6)$$

where M_{th} is the real value of the mass (which follows the theoretical PDF in Eq. (1)), M_{obs} is the observed mass and the relation between them is given by $M_{\text{obs}} = xM_{\text{th}}$, where x is distributed normally, $x \sim \mathcal{N}(1, \sigma^2)$, and $P_G = \frac{1}{\sqrt{2\pi\sigma^2}} e^{-(x-1)^2/2\sigma^2}$. For the calculations below we take a value of $\sigma = 0.05$ (a 5% relative mass error). For most of the mass range we consider for BBHs, this choice is conservative. However, as discussed in Ref. [82], this may prove to be an optimistic choice for low-mass events near the NS-BH transition where the error could be higher, as well as significantly asymmetric. We have verified that our conclusions are not sensitive to this choice, as long as the error is not considerably larger (i.e. within a factor of few). As will be explained in more detail below, the parameter most sensitive to the measurement uncertainty is the M_{gap} cutoff, and we discuss the implications of larger errors on its estimation in the Results section.

Secondly, in the Fisher analysis below, we use a logarithmically-binned BHMF measurement, with bins wide enough to ensure minimal cross-over between bins due to measurement errors (and again, the conclusions are not sensitive to the particular bin width used here).

C. The total number of detected merger events

The observable we consider in this work is the total number of detected merger events with a given BH mass (M_1 , the mass of the heavier BH in the 1D case, or the two masses M_1, M_2 in the 2D case). The theoretical prediction for this quantity, based on our model for the BH mass probability distribution function and the merger rate is given by

$$\frac{dN(M_1)}{dM_1} = 4\pi A_{M_1} P(M_1) \int_{M_{\text{gap}}}^{M_1} A_{M_2} P(M_2) dM_2$$

$$\times \int_0^{z_{\max}(M_1, M_2)} \frac{c\chi(z)^2 R(z)}{(1+z)H(z)} dz, \quad (7)$$

where A_{M_1} and A_{M_2} are the normalizations of the two PDFs in Eqs. (1) and (3); The upper limit on the redshift integral, $z_{\max}(M_1, M_2)$, is the maximum redshift up to which the merger of a BBH with masses M_1, M_2 can be detected with the experimental setup considered; $H(z)$ is the Hubble parameter and $\chi(z)$ is the comoving distance. To incorporate the measurement error, we use the observed PDFs, Eq. (6). In the 2D case, we use $dN(M_1, M_2)/dM_1 dM_2$, defined similarly to Eq. (7), only dropping the first integration.

D. Fisher matrix constraints

We will use the Fisher matrix formalism to study how well the BHMF parameters, the merger rate and the binary mass ratio can be constrained using GW measurements. This method assumes that the likelihood distribution of the parameter values is a multivariate Gaussian, centered on chosen fiducial values. The Fisher matrix $F_{\mu\nu}$ for a model with parameters p_μ is given by [83, 84]

$$F_{\mu\nu} = \sum_i \frac{1}{\sigma_i^2} \frac{\partial N_i}{\partial p_\mu} \frac{\partial N_i}{\partial p_\nu}, \quad (8)$$

where N_i is the number of events in each mass bin i

$$N_i = \int_{M_{\min,i}}^{M_{\max,i}} \frac{dN(M_1)}{dM_1} dM_1 \quad (9)$$

is the number of detected BHs in a mass bin with edges $[M_{\min,i}, M_{\max,i}]$. In our analysis below we divide $N(M_1)$ into 30 logarithmic bins from $M_1 = 4$ to $M_1 = 120$. We assume the bins obey Poisson statistics and take $\sigma_i^2 = N_i$ as the expected variance in N_i . As long as the bins are wide enough and we have ample statistics, this should be a reasonable assumption. The Fisher matrix computed from Eq. (8) can then be inverted to obtain the covariance matrix of the model parameters.

We compute the Fisher matrix using the six parameters introduced earlier: the three BHMF parameters, $\{\alpha, M_{\text{gap}}, M_{\text{cap}}\}$, the two merger rate parameters, $\{R_a, R_b\}$, and the power-law index β of the mass ratio distribution. Our fiducial choice of parameter values is $\alpha = 2.35$, $M_{\text{gap}} = 5 M_\odot$, $M_{\text{cap}} = 60 M_\odot$, $R_a = 97 \text{ Gpc}^{-3} \text{ yr}^{-1}$, $R_b = 2$ and $\beta = 0$. As we explain below, depending on the desired forecast, in some cases we focus on certain parameters and marginalize over the value of others. The cosmological parameters that enter our calculations are taken from Ref. [85]. Finally, we note that when addressing the 2D mass distribution, the formalism is almost identical. We simply replace $N(M_1)$ with $N(M_1, M_2)$, divide into 15×15 bins and N_i is then the number of BHs in each 2D mass bin.

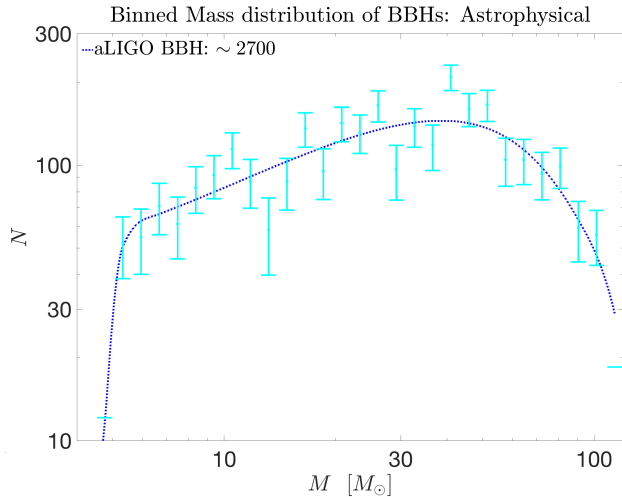


FIG. 2. The logarithmically-binned distribution of the mass of the heavier component in BBH mergers with 2700 BHs (as predicted for 6 years of aLIGO at final design sensitivity given our noise assumptions). The dashed blue line shows the theoretical expectation with our set of fiducial parameters, and the cyan error bars indicate the expected distribution assuming $\sqrt{N_i}$ Poisson noise in each mass bin.

IV. RESULTS

Our first result is a calculation of the number of observed events as a function of the mass of the heavier member of the BBH, given in Eq. (7). In Fig. 2 we plot the predicted mass distribution of observed BBH mergers for six years of advanced LIGO observations (at design sensitivity), which totals ~ 2700 events for our choice of parameters. As we can see, this function has a peak at masses much heavier than the peak of the PDF in Fig. (1). This peak is in fact very close to the mass of the heavier BH in the first event detected by LIGO, $M_1 \sim 36 M_\odot$. This stems from the fact that heavier masses yield mergers with larger GW strain amplitudes, and can therefore be detected at greater luminosity distances. The resulting increase in detectable *volume* is more than enough to compensate for the negative mass function slope $-\alpha = -2.35$.

The number of expected GW events depends on the choice of both the lower mass cutoff M_{gap} and the upper cutoff M_{cap} . It also naturally depends on the assumed rate of merger events throughout the observable redshift volume². In our results below we investigate the degeneracies between the BHMF, the coalescence event rate and binary mass ratio parameters.

² We note that the fiducial rate we use, calculated in Ref. [31], relies on specific assumptions regarding the BHMF parameters. Thus if the true values of the latter deviate significantly from the ones assumed here, then the rate of $97 \text{ Gpc}^{-3}\text{yr}^{-1}$ would also have to be replaced. We neglect this subtlety in our analysis.

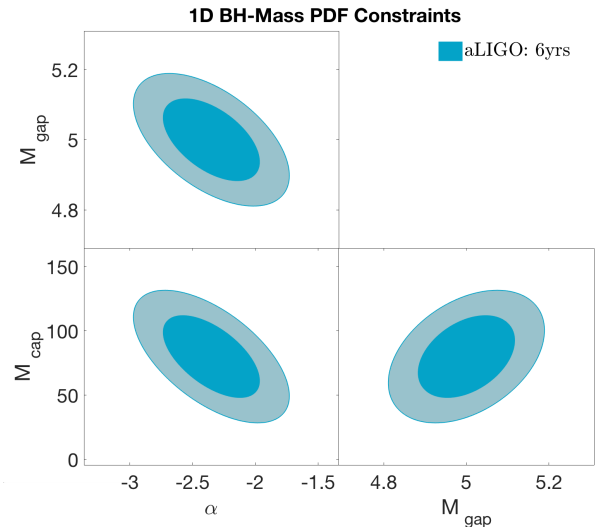


FIG. 3. Constraints on the BHMF parameters with 2,700 BHs (6 years of aLIGO observations). We marginalize over the merger rate parameters and over the value of the mass ratio power-law. The resulting constraints are promising. The constraint on α is tighter than the current best constraint on the IMF power law, while the lower mass cutoff can be measured well enough to confidently confirm or rule out a NS-BH mass gap.

Employing the Fisher analysis described above, we use this prediction for the observed mass distribution of the heavier black hole to calculate the resulting constraints on the three BHMF parameters. These are shown in Fig. 3. Here we marginalize over the merger rate parameters (we return to the merger rate below). From Fig. 3, we see that the detection of ~ 2700 events will yield constraints on the BHMF parameters ranging from 2% to 40% (at $1\text{-}\sigma$). The excellent sensitivity to the mass gap M_{gap} is such that if the true minimum mass of stellar black holes is indeed $\sim 5 M_\odot$, then we can reject the hypothesis that the distribution extends all the way down to the upper limit on neutron star masses of $\simeq 2 M_\odot$, with high significance ($\gg 5\sigma$). The sensitivity to the mass gap depends, however, on both the value of the cutoff and the assumed measurement error, which in practice may be asymmetric and larger on the low-mass end. If the cutoff is $M_{\text{gap}} = 4$, we will only be able to confirm the gap at the $\gtrsim 3\sigma$ level, unless the measurement error can be reduced to $< 5\%$ (and if the cutoff is even lower, it may remain undetectable until a more sensitive future experiment provides much more statistics). A $\gtrsim 3\sigma$ level of confidence will also correspond to a case where $M_{\text{gap}} = 5$ and the measurement error is $> 10\%$ in this mass range.

The BHMF power-law α is constrained to roughly 15%, which will suffice to detect considerable deviations from the power-law index of the IMF that could hint at possible selection effects in the black hole formation mechanism. The constraints on the top end of the distribution are weaker still, governed by the tradeoff between the

decreasing probability to see heavier masses versus the increase in signal to noise of their merger events. This weaker constraint is also a result of the fact that our model uses an exponential upper cutoff, which decays fairly slowly compared to sharper cutoffs, like we use for the lower mass end.

It is important to reemphasize that in the calculations above we also marginalized over the mass ratio between the two masses in each binary (the mass of the second black hole in each merger enters the calculation above indirectly as it affects its detectability). Therefore, as we use only the heavier mass measurements, we are discarding half(!) of the data at our disposal. However, as the mass of the lighter black hole in the binary tends to be highly dependent on its counterpart in many of the progenitor models, this ensures that the BHMF constraints we achieve are less model-dependent.

In the second part of this section we turn our focus to the two dimensional distribution, and show that in fact one could use the complete dataset, i.e. the two-dimensional mass distribution, precisely to distinguish between different progenitor models, as well as improving the constraints overall.

In Fig. 4 we plot the 2D mass distribution of BBH mergers, comparing the results for $\beta = -1, 0, 1$, which would correspond qualitatively to different (and distinct) progenitor models, as explained in the previous Section. Comparing the number counts along the diagonal and in the bottom corner of these plots, it is evident that information lost in the projection to the 1D M_1 -analysis can be used to improve the sensitivity to the mass ratio.

In Fig. 5, we compare the constraining power of the 1D and 2D distributions on the mass ratio. We see that the 2D information provides more than an order-of-magnitude improvement in the determination of the mass-ratio parameter β . On the other hand, the 2D BH mass distribution affects the precision with which we can measure the mass slope α only at the 30% level, and has a negligible effect on the precision of M_{gap} and M_{cap} . This behavior should not come as a surprise. The parameter β describes the PDF of the mass ratio M_2/M_1 . When using the 1D BH mass distribution, we are ignoring the information on M_2 that is then reintroduced in the 2D case. Evidently, to probe the progenitors of the BBHs we need the information on both M_1 and M_2 . The combined uncertainty on the BHMF is shown in Fig. 6.

We now return to the merger rate. It is clear that the mass ratio is degenerate with the rate of BBH mergers (a higher β yields more observed events, as mergers between higher masses are easier to detect), but as we shall advocate, the 2D information can be used to break this degeneracy. Fig. 7 demonstrates the degeneracy and also shows how using the full 2D information is efficient in breaking it and allowing for tighter constraints to be set on both the merger rate and mass ratio.

Since advanced LIGO, similarly to other planned experiments, is expected to be iteratively improved throughout the coming decade, it is also interesting to

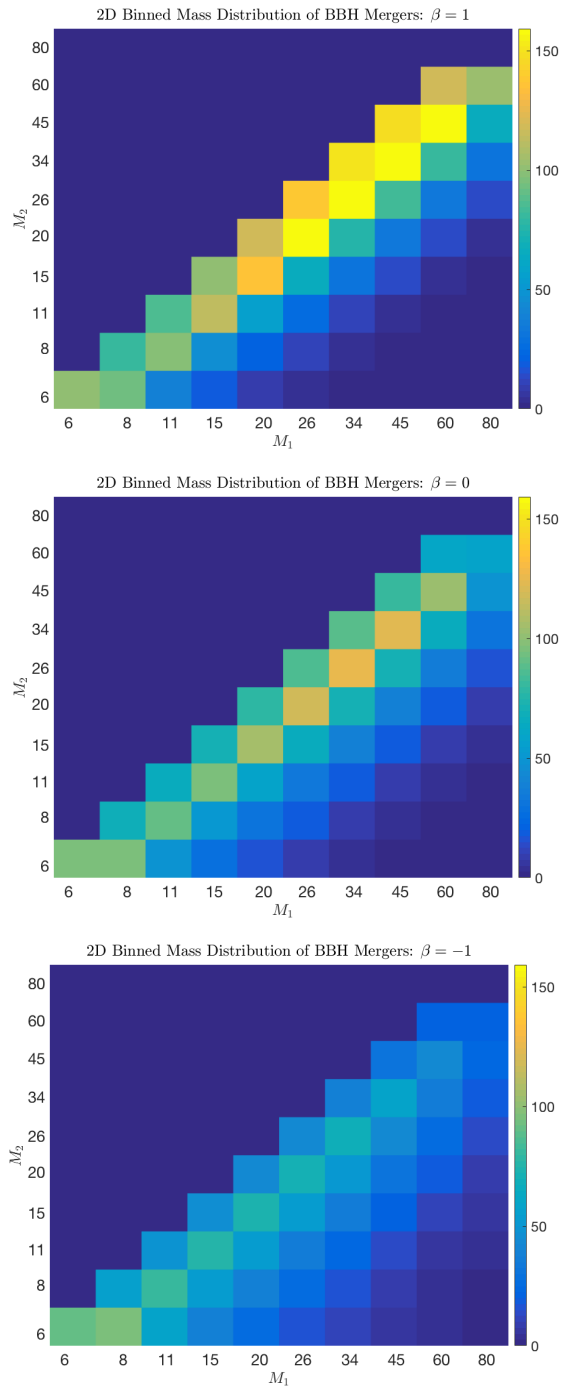


FIG. 4. The 2D mass distribution of BBH mergers, for three different mass-ratio power laws. While the projection of these plots down to one mass dimension would look qualitatively similar to Fig. 2, it is clear that the 2D mass distribution contains more information. This can be used to break degeneracies between parameters, as demonstrated in our subsequent results.

examine how the constraints inferred from the data will incrementally improve with increased observation time. In Table I, we present a full list of individual parameter

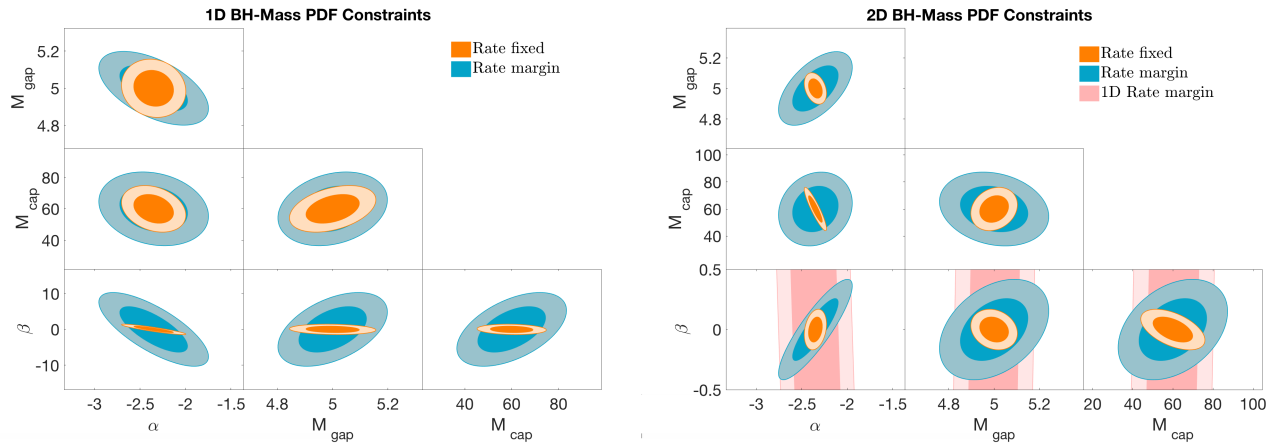


FIG. 5. Constraints on the BHMF parameters and the mass-ratio power law, using 1D and 2D data. While for measuring the BHMF parameters the improvement in going from one to two dimensions is modest, there is a stark difference in the constraints on the mass ratio parameter, which tighten by a factor ~ 20 . Note that the pink ellipses in the bottom right-hand plots (where the y-axis scale for β is much smaller) seem narrow, yet they do extend to a width similar to the blue ones when zooming out.

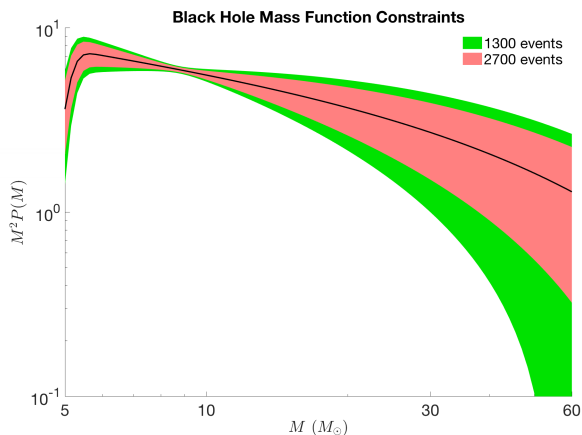


FIG. 6. Constraints on the BHMF, using 2D data.

constraints for a series of scenarios with respect to the observation time and imposed S/N detection threshold. We argue that the choice of detection threshold is an important point to consider. In the initial stages of GW exploration, as long as the focus is on singular merger events, it is prudent to limit the number of false detections considerably. However, when striving to acquire a large statistical ensemble of events, it might be worthwhile to lower the threshold and accept more events, even at the price of allowing for a few spurious events to be included in the dataset. This will introduce more noise in the mass distribution measurements, but as long as this is washed out by the Poisson noise in each mass bin, relaxing the bound may be preferred.

Finally, we end this section with an example of how the merging mass statistics can be used to probe particular models of binary progenitors. We focus on the primordial black hole model of [39], which was mentioned

above. In Fig. 8, we show a prediction for the mass spectrum of all detected merger events with advanced LIGO at design sensitivity, counting both stellar black holes and primordial ones (assuming the abundance of the latter is such that they make up the dark matter in the Universe). For the purpose of this exercise, we take a Gaussian centered at $30 M_\odot$ with a width of $3 M_\odot$ for the PBH mass function (models of PBH formation generally do not have clear predictions for the mass function, while current experimental constraints limit much wider distributions). As can be seen, with several years of LIGO data, a several- σ detection of PBHs can be made, or conversely a limit on the fraction of dark matter in PBHs can be inferred, assuming a particular form for the PBH mass function (conventionally, one adopts a delta-function mass function when calculating constraints of this type). This is consistent with the rough estimate in Ref. [39]. While other methods have been proposed to constrain PBH dark matter in the stellar-mass range [86–89], some even based on GW measurements [79, 90], we conclude that a simple examination of the mass spectrum is an efficient way of testing this scenario. We leave a more detailed investigation of this to future work [91].

V. DISCUSSION

Our analysis includes a few caveats that should be pointed out. Most evidently, a limitation of our results is that they rely on specific model choices, which include a (minimal) number of assumptions. For example, we assume a sharp cutoff at lower masses. This choice is motivated by both the currently available data (see Fig. 1) and by theoretical models of core-collapse supernovae whereby the instabilities driving the explosion have a rapid timescale (< 200 ms), which have been shown

Scenario	N	σ_α	$\sigma_{M_{\text{gap}}}(M_\odot)$	$\sigma_{M_{\text{cap}}}(M_\odot)$	σ_{R_a} ($\text{Gpc}^{-3}\text{yr}^{-1}$)	σ_{R_b}	σ_β
$S/N > 8$ and 1 years	440	0.41	0.24	27.29	43.46	3.65	0.42
$S/N > 8$ and 3 years	1330	0.23	0.14	15.75	25.09	2.11	0.24
$S/N > 8$ and 6 years	2670	0.17	0.10	11.14	17.74	1.49	0.17
$S/N > 10/\sqrt{2}$ and 6 years	3790	0.14	0.08	9.43	15.01	1.13	0.14
$S/N > 8/\sqrt{2}$ and 6 years	7050	0.11	0.06	7.87	11.85	0.72	0.11

TABLE I. Individual $1\text{-}\sigma$ constraints on the BHMF, the merger rate and the mass ratio parameters, under different scenarios. In addition to the standard criterion adopted by the LIGO collaboration of a signal-to-noise threshold *per detector* of 8, we also consider thresholds of either 10 or 8 for two detectors combined. Lower thresholds yield larger statistical ensembles, obviously. For comparison, fiducial values in our analysis were taken to be $\alpha = 2.35$, $M_{\text{gap}} = 5M_\odot$, $M_{\text{cap}} = 60M_\odot$, $R_a = 97 \text{ Gpc}^{-3}\text{yr}^{-1}$, $R_b = 2$ and $\beta = 0$. We treat 1 year of observation as 365 full days of data collection (duty cycle of unity).

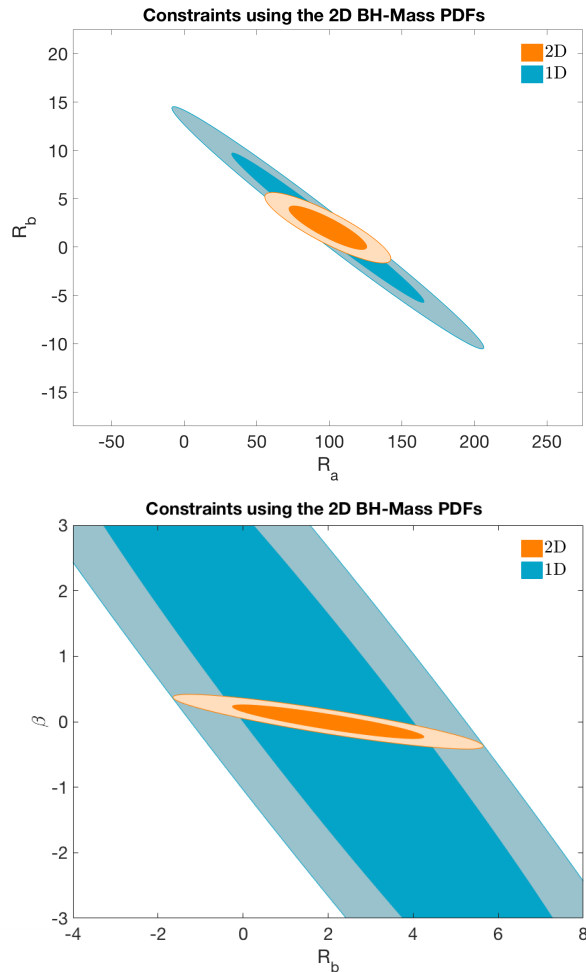


FIG. 7. *Top*: Constraints on the merger rate parameters, using 1D and 2D data (marginalizing over the other parameters). *Bottom*: The joint constraints for the mass-ratio power law and the merger-rate power law, showing the strong degeneracy, which is then broken quite effectively when using the 2D information.

to exhibit a NS-BH mass gap [10, 38]. Nevertheless, it would be interesting to consider other choices, especially

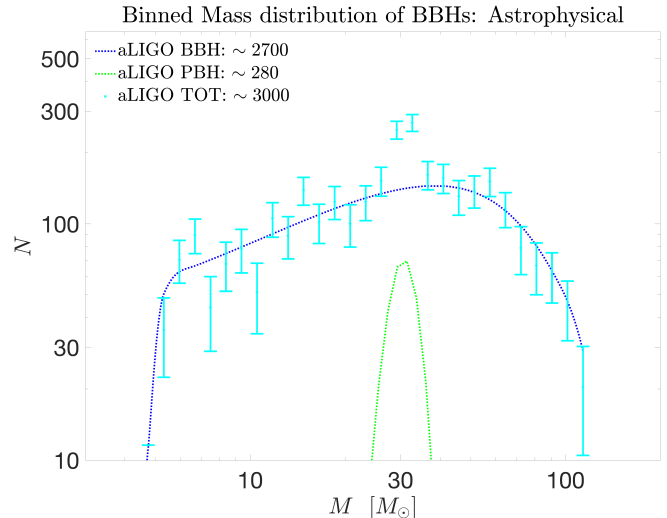


FIG. 8. The logarithmically-binned distribution of the mass of the heavier component in BBH mergers, including mergers of both stellar black hole and primordial black holes (with a merger rate consistent with the assumption that they make up all of dark matter in the Universe, see Ref. [39]).

as more data is collected and the shape of the BHMF at low masses begins to unveil itself.

Another assumption we have made is that the BBH merger rate is mass-independent. While this assertion is supported in some models which take into account the explosion mechanism, the metallicity history and the time delay distribution (see e.g. [10, 92]), it presents a source of additional uncertainty. In follow up work, our analysis can be extended by incorporating the dependence of the merger rate on both mass and metallicity, and following the cosmic history of star formation and metallicity distribution, as well as the distribution of the delay time between formation and merger of the binaries. This can be done in the context of a galaxy evolution model, as carried out in Ref. [93], for example. This model currently assumes that the two masses in each binary have

independent distributions. It would be intriguing to generalize this method, accounting for different progenitor scenarios and incorporating the corresponding expectations for the mass ratio, and then proceed to investigate how well these models can be probed with future measurements.

We have focused on mass measurements in this work, neglecting the spin of the black holes³. There is definitely motivation to consider how well the distribution of initial spins of the merging black holes can be measured with future data, and make the connection with theoretical predictions. We leave this for future work.

We have also not included any discussion regarding systematic bias in the parameter estimation of individual BBH coalescence events. In Ref. [94], it was shown that for events with $\text{SNR} < 50$ (applicable for LIGO), any bias in characterizing the GW events, introduced by the use of current waveforms, remains within the relevant statistical errors associated with the widths of the posterior distribution functions. More recently, in [95], it was also shown that even if the location on the sky and the distance to the binary are well known, either using an electromagnetic counterpart signal, or in the future by previous observations of the system [96] with eLISA [97], the accuracy in measuring the spins and masses of the binary BHs does not improve significantly. As more observations are gathered with the gradual improvement of the LIGO detectors, it may be worthwhile to repeat the analysis done here, reflecting our lessons regarding the operating sensitivity of the instrument and the fiducial parameter values we used. Given the current uncertainties, our order of magnitude estimations are adequate.

Care should be taken when directly comparing our results with forecasts made by the LIGO collaboration and others. Beyond specific choices of parameters, which should not lead to any qualitative differences, we also ignore the fact that when searching for GW events in the LIGO data, the current bank of GW waveforms contains certain limitations, such as a total mass limit of $M_1 + M_2 < 100 M_\odot$ [31]. Such massive events, however, will yield very powerful signatures and may still be detected via the burst trigger or wavelet template searches. To facilitate the comparison with Ref. [31], we adopted the same value for the low mass cutoff. As also noted in Ref. [31], however, the total number of observed black holes in a given observation time will depend on this choice (the fixed fiducial merger rate amplitude we set means that a lower mass cutoff will result in a smaller abundance of more massive BHs, which are also more easily detectable).

Lastly, we advocated that it may be worthwhile to lower the S/N threshold imposed on the merger candidates identified by the template fitting process in order to

enlarge the statistical ensemble used for inference of the BHMF and mass ratio parameters. Table I demonstrates the potential gain from a larger sample of BHs. However, it is important to emphasize that our analysis does not model the trigger events and does not account for any systematics or uncertainties that may be introduced by this process, which are beyond the scope of this paper.

Before concluding, it is worth mentioning other approaches that have been proposed to measure the black hole mass function. One such method is to attempt to detect the formation of black holes by monitoring millions of supergiants and searching for the disappearance of massive stars, indicating the occurrence of failed supernovae [98]. This is an ongoing effort [99, 100] which will greatly improve with future instruments such as WFIRST [101]. While this method does not directly measure the black hole mass, it does offer insight as to which stars end up becoming black holes and what is the likely final black hole mass. Another promising method, which does target the black hole masses themselves, is to look for black holes via microlensing (their gravitational lensing effect on background stars), as proposed in Ref. [102] and recently attempted in Ref. [103]. Techniques such as these circumvent the uncertainty introduced by the detailed physics of binary formation and evolution in gravitational wave measurements of merging black holes, but will likely suffer from various selection effects of their own.

VI. CONCLUSIONS

In this work we have investigated how measurements of gravitational waves from the merger of BBHs stand to advance our understanding of the mass distribution of BHs, thereby opening a completely new avenue to study the most basic motif in astrophysics, namely the physics of stars, as well as provide us with valuable information about their cosmic history. In order to assess the power of a large statistical ensemble of mass measurements, it was important to adopt a well-motivated model for the BHMF, the BBH merger rate and the binary mass ratio, and to properly take into account important ingredients such as the instrumental noise and the mass measurement errors. Doing so, we attained a prediction for the number of detected events as a function of the mass of the constituent black holes.

An immediate conclusion this approach enabled, for example, is that events with masses in a range similar to those of the first event detected by advanced LIGO (and considerably more massive than the previously known BHs from X-ray observations), are in fact the most likely to be detected by this experiment (see Figure 2).

We then proceeded to study in detail how well the BHMF, the mass ratio, and the merger rate can be constrained with future data. We found that once LIGO reaches its design sensitivity, an expected number of $\gtrsim 400$ black hole mergers will be observed per year, yielding remarkable constraints on the BHMF parame-

³ In calculating Eq. (7), we set α_f , the final spin parameter (which affects the result of $z_{\max}(M_1, M_2)$), to 0.67 for all merger events. Relaxing this assumption, however, has a negligible effect.

ters. Notably, it will allow a measurement of the BHMF power law to better accuracy than our current best constraints on the stellar IMF power law in the heavier mass tail. By the time advanced LIGO finishes its planned full run, less than a decade from now, these constraints will more than double in accuracy. Together with the increasingly tight bound on the higher mass end of the BHMF, which probes the efficiency with which the heaviest stars maintain their mass, these results may therefore have more to say about the stellar mass distribution than the measurements of stars themselves(!).

The excellent expected sensitivity to the mass gap M_{gap} , as indicated by our results, is such that if the true minimum mass of stellar black holes is indeed $\sim 5 M_{\odot}$, as indicated by (the very limited number of) current observations, then we can reject the hypothesis that the distribution extends all the way down to the upper limit on neutron star masses of $\simeq 2 M_{\odot}$ at high significance. The uncertainty on the upper limit to stellar BH masses is expected to decrease to less than a decade in mass by the end of the LIGO run, providing an (indirect) observational handle on stars in their Wolf-Rayet phase.

Another important conclusion of this work is that in order to exhaust the information from the mass measurements of merging black holes, it is imperative to focus on the two-dimensional mass distribution (of M_1 and M_2), shown in Fig. 4. This provides sensitivity to the progenitor models and breaks degeneracies between the merger rate and BHMF parameters and the binary mass ratio, as shown in Fig. 5. We demonstrated that the effect of the merger rate parameters and the mass ratio on the observed mass distribution are tightly connected, and showed that the constraints on the mass ratio improve by more than an order of magnitude when using the full 2D information (see Fig. 7). When modeled as a power law, advanced LIGO should yield better than 10% constraints on the value of β , its power law index (see Table I).

These findings thus leave room for more detailed modeling of the BH progenitor mechanisms—and the interplay between them—to be efficiently probed with the advent of thousands of GW detections from BH mergers. Future work will also consider next generation detectors such as the proposed Einstein Telescope [104], which can reach much greater sensitivities and would therefore probe the binary formation and merger history into higher redshifts, enabling tests of more extensive models than considered here. Finally, the more exotic example discussed above, of primordial black holes, provides a proof-of-concept that GW measurements can be used to derive constraints on the primordial spectrum of fluctuations which is imprinted onto the early Universe over cosmological scales by cosmological inflation [105, 106]. This is another exciting topic to be studied in future work.

In conclusion, our results demonstrate that gravitational wave astronomy in the next decade will open up a novel and unique observational window on our Universe. If treated with the appropriate tools, as suggested above, this information can provide unprecedented insights into the physics of black hole formation, the survival of heavy stars, the history of star formation, the explosion mechanism of core-collapse supernovae, the nature of binary black hole progenitors, and even the existence of peaks in the primordial power spectrum of density fluctuations. Clearly, measurements of black holes will be enlightening.

ACKNOWLEDGMENTS

We thank Yacine Ali-Haïmoud, Bruce Allen, Simeon Bird, Irina Dvorkin, Julian Muñoz and Joe Silk for useful discussions. IC thanks the organizers of the GW & Cosmology workshop in DESY, Hamburg, Germany. This work was supported by NSF Grant No. 0244990, NASA NNX15AB18G and the Simons Foundation.

-
- [1] K. Schwarzschild, Sitzungsber. Preuss. Akad. Wiss. Berlin (Math. Phys.) **1916**, 189 (1916), physics/9905030.
 - [2] J. R. Oppenheimer and H. Snyder, Phys. Rev. **56**, 455 (1939).
 - [3] M. M. May and R. H. White, Phys. Rev. **141**, 1232 (1966).
 - [4] H. A. Bethe, Reviews of Modern Physics **62**, 801 (1990).
 - [5] H.-T. Janka, Ann. Rev. Nucl. Part. Sci. **62**, 407 (2012), 1206.2503.
 - [6] C. L. Fryer, Astrophys. J. **522**, 413 (1999), astro-ph/9902315.
 - [7] C. L. Fryer and V. Kalogera, Astrophys. J. **554**, 548 (2001), astro-ph/9911312.
 - [8] E. O'Connor and C. D. Ott, Astrophys. J. **730**, 70 (2011), 1010.5550.
 - [9] B. P. Abbott et al. (Virgo, LIGO Scientific), Astrophys. J. **818**, L22 (2016), 1602.03846.
 - [10] C. L. Fryer, K. Belczynski, G. Wiktorowicz, M. Dominik, V. Kalogera, and D. E. Holz, Astrophys. J. **749**, 91 (2012), 1110.1726.
 - [11] C. Motch, F. Haberl, K. Dennerl, M. Pakull, and E. Janot-Pacheco, Astron. Astrophys. **323**, 853 (1997), astro-ph/9611122.
 - [12] J. J. M. in't Zand et al., Astron. Astrophys. **357**, 520 (2000), astro-ph/0001110.
 - [13] H. J. Grimm, M. Gilfanov, and R. Sunyaev, Astron. Astrophys. **391**, 923 (2002), astro-ph/0109239.
 - [14] A. Lutovinov, M. Revnivtsev, M. Gilfanov, P. Shtykovskiy, S. Molkov, and R. Sunyaev, Astron. Astrophys. **444**, 821 (2005), astro-ph/0411550.
 - [15] R. Corbet et al. (Swift BAT), Prog. Theor. Phys. Suppl. **169**, 200 (2007), astro-ph/0703274.
 - [16] D. M. Russell et al., Astrophys. J. **768**, L35 (2013), 1304.3510.

- [17] J. M. Corral-Santana, J. Casares, T. Muñoz-Darias, F. E. Bauer, I. G. Martínez-Pais, and D. M. Russell, *Astron. Astrophys.* **587**, A61 (2016), 1510.08869.
- [18] A. I. Bogomazov (2016), 1607.03358.
- [19] P. C. Peters and J. Mathews, *Phys. Rev.* **131**, 435 (1963).
- [20] P. C. Peters, *Phys. Rev.* **136**, B1224 (1964).
- [21] L. Blanchet, *Living Rev. Rel.* **5**, 3 (2002), gr-qc/0202016.
- [22] E. Berti, V. Cardoso, and A. O. Starinets, *Class. Quant. Grav.* **26**, 163001 (2009), 0905.2975.
- [23] P. Ajith, *Phys. Rev.* **D84**, 084037 (2011), 1107.1267.
- [24] J. Frank and M. J. Rees, *Mon. Not. Roy. Astron. Soc.* **176**, 633 (1976).
- [25] J. S. Bloom et al., *Science* **333**, 203 (2011), 1104.3257.
- [26] N. Stone, R. Sari, and A. Loeb, *Mon. Not. Roy. Astron. Soc.* **435**, 1809 (2013), 1210.3374.
- [27] Y. Ali-Haïmoud, E. D. Kovetz, and J. Silk, *Phys. Rev.* **D93**, 043508 (2016), 1511.02232.
- [28] A. Einstein, *Sitzungsber. Preuss. Akad. Wiss. Berlin (Math. Phys.)* **1918**, 154 (1918).
- [29] B. P. Abbott et al. (Virgo, LIGO Scientific), *Phys. Rev. Lett.* **116**, 061102 (2016), 1602.03837.
- [30] B. P. Abbott et al. (Virgo, LIGO Scientific), *Phys. Rev. Lett.* **116**, 241103 (2016), 1606.04855.
- [31] B. P. Abbott et al. (Virgo, LIGO Scientific) (2016), 1606.04856.
- [32] F. Acernese et al. (VIRGO), *Class. Quant. Grav.* **32**, 024001 (2015), 1408.3978.
- [33] Y. Aso, Y. Michimura, K. Somiya, M. Ando, O. Miyakawa, T. Sekiguchi, D. Tatsumi, and H. Yamamoto (KAGRA), *Phys. Rev.* **D88**, 043007 (2013), 1306.6747.
- [34] <http://gwcenter.icrr.u.tokyo.ac.jp/en/>.
- [35] <http://www.gw-indigo.org/ligo/india>.
- [36] F. Ozel, D. Psaltis, R. Narayan, and J. E. McClintock, *Astrophys. J.* **725**, 1918 (2010), 1006.2834.
- [37] W. M. Farr, N. Sravan, A. Cantrell, L. Kreidberg, C. D. Baily, I. Mandel, and V. Kalogera, *Astrophys. J.* **741**, 103 (2011), 1011.1459.
- [38] K. Belczynski, G. Wiktorowicz, C. Fryer, D. Holz, and V. Kalogera, *Astrophys. J.* **757**, 91 (2012), 1110.1635.
- [39] S. Bird, I. Cholis, J. B. Muñoz, Y. Ali-Haïmoud, M. Kamionkowski, E. D. Kovetz, A. Raccanelli, and A. G. Riess, *Phys. Rev. Lett.* **116**, 201301 (2016), 1603.00464.
- [40] J. M. Corral-Santana, J. Casares, T. Muñoz-Darias, P. Rodriguez-Gil, T. Shahbaz, M. A. P. Torres, C. Zurita, and A. A. Tyndall, *Science* **339**, 1048 (2013), 1303.0034.
- [41] J. Casares and P. G. Jonker, *Space Sci. Rev.* **183**, 223 (2014), 1311.5118.
- [42] J. A. Orosz et al., *Astrophys. J.* **697**, 573 (2009), 0810.3447.
- [43] J. F. Steiner, J. E. McClintock, J. A. Orosz, R. A. Remillard, C. D. Baily, M. Kolehmainen, and O. Straub, *Astrophys. J.* **793**, L29 (2014), 1402.0148.
- [44] A. K. F. Val-Baker, A. J. Norton, and I. Negueruela, in *AIPC 924 530V 2007* (2016), vol. 924, p. 530, 1608.01187.
- [45] J. A. Orosz et al., *Nature* **449**, 872 (2007), 0710.3165.
- [46] J. M. Silverman and A. V. Filippenko, *Astrophys. J.* **678**, L17 (2008), 0802.2716.
- [47] E. E. Salpeter, *Astrophys. J.* **121**, 161 (1955).
- [48] P. Kroupa, *Mon. Not. Roy. Astron. Soc.* **322**, 231 (2001), astro-ph/0009005.
- [49] T. Sukhbold, T. Ertl, S. E. Woosley, J. M. Brown and H.-T. Janka, *Astrophys. J.* **821**, no. 1, 38 (2016) [arXiv:1510.04643 [astro-ph.HE]].
- [50] O. Pejcha and T. A. Thompson, *Astrophys. J.* **801**, no. 2, 90 (2015) [arXiv:1409.0540 [astro-ph.HE]].
- [51] Kochanek, C. S. 2015, *Mon. Not. R. Astron. Soc.*, 446, 1213
- [52] D. Clausen, A. L. Piro and C. D. Ott, *Astrophys. J.* **799**, no. 2, 190 (2015) [arXiv:1406.4869 [astro-ph.HE]].
- [53] J. M. Lattimer, *Ann. Rev. Nucl. Part. Sci.* **62**, 485 (2012), 1305.3510.
- [54] J. Antoniadis et al., *Science* **340**, 6131 (2013), 1304.6875.
- [55] A. V. Filippenko, D. C. Leonard, T. Matheson, W. Li, E. C. Moran, and A. G. Riess, *Publ. Astron. Soc. Pac.* **111**, 969 (1999), astro-ph/9904271.
- [56] C. D. Baily, R. K. Jain, P. Coppi, and J. A. Orosz, *Astrophys. J.* **499**, 367 (1998), astro-ph/9708032.
- [57] L. Kreidberg, C. D. Baily, W. M. Farr, and V. Kalogera, *Astrophys. J.* **757**, 36 (2012), 1205.1805.
- [58] C. S. Kochanek, *Astrophys. J.* **785**, 28 (2014), 1308.0013.
- [59] P. A. Crowther, *Ann. Rev. Astron. Astrophys.* **45**, 177 (2007), astro-ph/0610356.
- [60] N. Smith, *Ann. Rev. Astron. Astrophys.* **52**, 487 (2014), 1402.1237.
- [61] P. A. Crowther, O. Schnurr, R. Hirschi, N. Yusof, R. J. Parker, S. P. Goodwin, and H. A. Kassim, *Mon. Not. Roy. Astron. Soc.* **408**, 731 (2010), 1007.3284.
- [62] S. Komossa and H. Schulz, *Astron. Astrophys.* **339**, 345 (1998), astro-ph/9810174.
- [63] C. Weidner and P. Kroupa, *Mon. Not. Roy. Astron. Soc.* **348**, 187 (2004), astro-ph/0310860.
- [64] C. Koen, *Mon. Not. R. Astron. Soc.* **365**, 590 (2006).
- [65] M. S. Oey and C. J. Clarke, *Astrophys. J.* **620**, L43 (2005), astro-ph/0501135.
- [66] S. Banerjee, P. Kroupa, and S. Oh, *Astrophys. J.* **746**, 15 (2012), 1111.0291.
- [67] L. Rizzi, F. Bresolin, R.-P. Kudritzki, W. Gieren, and G. Pietrzynski, *Astrophys. J.* **638**, 766 (2006), astro-ph/0510298.
- [68] B. P. Abbott et al. (Virgo, LIGO Scientific), *Class. Quant. Grav.* **33**, 134001 (2016), 1602.03844.
- [69] J. Aasi et al. (VIRGO, LIGO Scientific) (2013), [Living Rev. Rel.19,1(2016)], 1304.0670.
- [70] B. Sathyaprakash et al., in *2011 Gravitational Waves and Experimental Gravity, The Gioi Publishers, Vietnam* (2011), 1108.1423.
- [71] M. Dominik, K. Belczynski, C. Fryer, D. E. Holz, E. Berti, T. Bulik, I. Mandel, and R. O'Shaughnessy, *Astrophys. J.* **779**, 72 (2013), 1308.1546.
- [72] K. Belczynski, V. Kalogera, and T. Bulik, *Astrophys. J.* **572**, 407 (2001), astro-ph/0111452.
- [73] S. E. Woosley, N. Langer, and T. A. Weaver, *Astrophys. J.* **448**, 315 (1995).
- [74] P. Marchant, N. Langer, P. Podsiadlowski, T. M. Tauris, and T. J. Moriya, *Astron. Astrophys.* **588**, A50 (2016), 1601.03718.
- [75] R. M. O'Leary, Y. Meiron, and B. Kocsis, *Astrophys. J.* **824**, L12 (2016), 1602.02809.
- [76] C. L. Rodriguez, S. Chatterjee, and F. A. Rasio, *Phys. Rev.* **D93**, 084029 (2016), 1602.02444.

- [77] S. Sigurdsson and L. Hernquist, *Nature* **364**, 423 (1993).
- [78] C. L. Rodriguez, C.-J. Haster, S. Chatterjee, V. Kalogera, and F. A. Rasio, *Astrophys. J.* **824**, L8 (2016), 1604.04254.
- [79] I. Cholis, E. D. Kovetz, Y. Ali-Haïmoud, S. Bird, M. Kamionkowski, J. B. Muñoz, and A. Raccanelli, *Phys. Rev.* **D94**, 084013 (2016), 1606.07437.
- [80] J. Abadie et al. (VIRGO, LIGO Scientific), *Class. Quant. Grav.* **27**, 173001 (2010), 1003.2480.
- [81] D. Shoemaker, <https://dcc.ligo.org/public/0002/T0900288/003/AdvLIGOnoise20curves.pdf> (2010).
- [82] M. Hannam, D. A. Brown, S. Fairhurst, C. L. Fryer and I. W. Harry, *Astrophys. J.* **766**, L14 (2013) [arXiv:1301.5616 [gr-qc]].
- [83] G. Jungman, M. Kamionkowski, A. Kosowsky, and D. N. Spergel, *Phys. Rev. Lett.* **76**, 1007 (1996), astro-ph/9507080.
- [84] G. Jungman, M. Kamionkowski, A. Kosowsky, and D. N. Spergel, *Phys. Rev.* **D54**, 1332 (1996), astro-ph/9512139.
- [85] P. A. R. Ade et al. (Planck), *Astron. Astrophys.* **594**, A13 (2016), 1502.01589.
- [86] E. Mediavilla, J. A. Munoz, E. Falco, V. Motta, E. Guerras, H. Canovas, C. Jean, A. Oscoz, and A. M. Mosquera, *Astrophys. J.* **706**, 1451 (2009), 0910.3645.
- [87] J. B. Muñoz, E. D. Kovetz, L. Dai, and M. Kamionkowski, *Phys. Rev. Lett.* **117**, 091301 (2016), 1605.00008.
- [88] T. D. Brandt, *Astrophys. J.* **824**, L31 (2016), 1605.03665.
- [89] K. Schutz and A. Liu (2016), 1610.04234.
- [90] A. Raccanelli, E. D. Kovetz, S. Bird, I. Cholis, and J. B. Muñoz, *Phys. Rev.* **D94**, 023516 (2016), 1605.01405.
- [91] E. D. Kovetz et al., in preparation (2016).
- [92] I. Dvorkin, E. Vangioni, J. Silk, J.-P. Uzan, and K. A. Olive (2016), 1604.04288.
- [93] I. Dvorkin, J.-P. Uzan, E. Vangioni, and J. Silk (2016), 1607.06818.
- [94] T. B. Littenberg, J. G. Baker, A. Buonanno, and B. J. Kelly, *Phys. Rev.* **D87**, 104003 (2013), 1210.0893.
- [95] C. Pankow, L. Sampson, L. Perri, E. Chase, S. Coughlin, M. Zevin, and V. Kalogera (2016), 1610.05633.
- [96] A. Sesana, *Phys. Rev. Lett.* **116**, 231102 (2016), 1602.06951.
- [97] P. Amaro-Seoane et al., *Class. Quant. Grav.* **29**, 124016 (2012), 1202.0839.
- [98] C. S. Kochanek, J. F. Beacom, M. D. Kistler, J. L. Prieto, K. Z. Stanek, T. A. Thompson and H. Yuksel, *Astrophys. J.* **684**, 1336 (2008) [arXiv:0802.0456 [astro-ph]].
- [99] S. M. Adams, C. S. Kochanek, J. R. Gerke and K. Z. Stanek, arXiv:1610.02402 [astro-ph.SR].
- [100] S. M. Adams, C. S. Kochanek, J. R. Gerke, K. Z. Stanek and X. Dai, arXiv:1609.01283 [astro-ph.SR].
- [101] Spergel, D., Gehrels, N., Baltay, C., et al. 2015, arXiv:1503.03757
- [102] A. Gould, *Astrophys. J.* **535**, 928 (2000) [astro-ph/9906472].
- [103] Lu, J. R., Sinukoff, E., Ofek, E. O., Udalski, A., & Kozłowski, S. 2016, *Astrophys. J.*, 830, 41
- [104] B. Sathyaprakash et al., *Class. Quant. Grav.* **29**, 124013 (2012), 1206.0331.
- [105] B. Carr, F. Kuhnel, and M. Sandstad, *Phys. Rev.* **D94**, 083504 (2016), 1607.06077.
- [106] J. B. Muñoz, E. D. Kovetz, A. Raccanelli, M. Kamionkowski, and J. Silk, in preparation (2016).